Distribution Agreement

In presenting this thesis as a partial fulfillment of the requirements for a degree from Emory University, I hereby grant to Emory University and its agents the non-exclusive license to archive, make accessible, and display my thesis in whole or in part in all forms of media, now or hereafter now, including display on the World Wide Web. I understand that I may select some access restrictions as part of the online submission of this thesis. I retain all ownership rights to the copyright of the thesis. I also retain the right to use in future works (such as articles or books) all or part of this thesis.

Zilu Pang   April 9, 2025

Investigating Thermal Transport in β-Ta: A Combined Noise and COMSOL Study

by

Zilu Pang

Sergei Urazhdin

Adviser

Department of Physics

Sergei Urazhdin

Adviser

Erin Bonning

Committee Member

Jed Brody

Committee Member

2025

Investigating Thermal Transport in β-Ta: A Combined Noise and COMSOL Study

By

Zilu Pang

Sergei Urazhdin
Adviser

An abstract of
a thesis submitted to the Faculty of Emory College of Arts and Sciences
of Emory University in partial fulfillment
of the requirements of the degree of
Bachelor of Science with Honors

Department of Physics

2025

Abstract

Investigating Thermal Transport in β-Ta: A Combined Noise and COMSOL Study
By Zilu Pang

This work investigates the thermal transport behavior of β-phase tantalum (β-Ta) at

cryogenic temperatures, focusing on the distinct roles of the metallic leads and the

substrate in heat dissipation. Using differential noise measurements, a low temperature

thermal conductivity model of the form $\kappa(T) = aT + bT^3$ was developed, capturing

the combined electron and phonon contribution of heat into the leads. Importantly,

we restricted our analysis to the thermal broadening region, where voltage bias

VB is less than crossover voltage Vth, allowing us to treat all measured noise as

thermal noise. However, the simple model for thermal conductivity through the leads

breaks down at 2μm length scale, so exploring thermal transport through insulating

substrate led us to COMSOL simulation. To visualize dissipation pathways within

the substrate, a COMSOL model incorporating Joule heating was implemented to

compute the temperature distribution across the β-Ta strip, copper leads, and sapphire

substrate. We further highlight the discrepancy between the simulated thermal noise

and experimental value to discuss thermal transport within a bad metal β-Ta at

nanoscale.

Investigating Thermal Transport in β-Ta: A Combined Noise and COMSOL Study

By

Zilu Pang

Sergei Urazhdin
Adviser

A thesis submitted to the Faculty of Emory College of Arts and Sciences
of Emory University in partial fulfillment
of the requirements of the degree of
Bachelor of Science with Honors

Department of Physics

2025

Acknowledgements

First, I express my deepest gratitude to my advisor, Professor Sergei Urazhdin, for

his invaluable guidance, patience, and support throughout this project. His insights

and encouragement have been instrumental in shaping my understanding of physics

and experimental research.

Special thanks go to Mateusz Szurek, whose mentorship has been truly transfor-

mative. He taught me everything from fundamental concepts to the smallest lab

techniques, and his patience and willingness to guide me through every challenge have

been invaluable. I am incredibly grateful for the time and effort he has dedicated to

helping me grow as a researcher.

The author also wishes to thank Hanqiao Cheng, Yiou Zhang, and Sergei Ivanov

for their support, insightful discussions, and camaraderie in the lab. Your advice and

shared experiences have made this journey both productive and enjoyable.

I am sincerely grateful to my committee members, Professor Erin Bonning and

Professor Jed Brody for attending my defense. I appreciate their time and presence

to my research discussion.

Finally, I am thankful for all the friends, colleagues, and faculty members who

have contributed to my academic journey. This work would not have been possible

without their support and inspiration.

Table of Contents

List of Figures

List of Tables

Chapter 1

Introduction

1.1 Motivation

Efficient heat dissipation is a fundamental challenge in modern nanoscale electronics. As devices continue to scale down to microscopic in size while operating in high power densities, managing thermal energy becomes critical. In particular, exploring and understanding the heat transport mechanism in materials with unconventional electronic properties is essential in making next-generation devices.

Among all unconventional metals, tantalum is an important transition metal with an α phase and a β phase, a metastable phase that exhibits "bad metal" metallic behaviors. Unlike α-Ta, which has well characterized thermal and electrical properties, β-Ta shows a relative high resistivity, making it a promising metal candidate for resistive elements in circuits such as a resistor, where high and stable resistance values are often desirable.

Moreover, a previous study by our group has reported suppressed shot noise detected in β-Ta nanowire, characterized by a reduced Fano factor. This finding suggests an underlying electron transport mechanism that is not yet fully understood [10]. This motivated our investigation into the thermal transport behavior of β-Ta,

especially the role of electrons and phonons in heat dissipation. Building upon these findings, this project aims to explore the thermal transport behavior of a bad metal, β-Ta, at cryogenic temperature using a combination of noise measurement and COMSOL Simulation. This project also serves as a probe to derive an expression for the thermal conductivity of a β-Ta nanowire and investigate thermal transport of a bad metal. This study aims to present the experimental observations and heat dissipation simulations in a nanoscale system while providing new insights into the relationship between phononic and electronic contributions. Understanding heat transport in bad metal might be crucial for nanoscale electronics.

1.2   Background

To contextualize the approaches of the study, this section provides a brief overview of the core concepts involved: bad metal, Johnson-Nyquist noise, shot noise, and the heat dissipation model.

1.2.1   Bad Metal

The material known as a "bad" metal exhibits relatively high resistivity, often approaching the Mott-Ioffe-Regel limit (MIR). In this regime, the mean free path of electrons is comparable or less than the lattice constant, so the well-defined quasiparticle picture breaks down.

β-Ta, a metastable phase of tantalum, falls precisely into this category. The Temperature Coefficient of Resistivity (TCR) plot generated by four-point probe measurement reveals a negative TCR trend as temperature increases according to Figure 1.1. The resistivity of β-Ta $\rho \sim 1-3\,\mu\Omega$·m almost satisfies the Mott-Ioffe-Regel limit (MIR), and it increases with decreasing temperature. Thus, the quasiparticle picture for β-Ta is questionable [3]. Moreover, the negative TCR observed in β-Ta is

a signature of strong disorder and is commonly attributed to weak localization effects [6]. As shown in Kovaleva et al. (2015), such behaviors can be further enhanced by electron correlations, suggesting that both localization and many-body effects potentially contribute to the non-metallic transport characteristics in disorder β-Ta thin films. Therefore, β-Ta's anomalous transport properties make it a particularly compelling example of a "bad metal" worthy of detailed study.
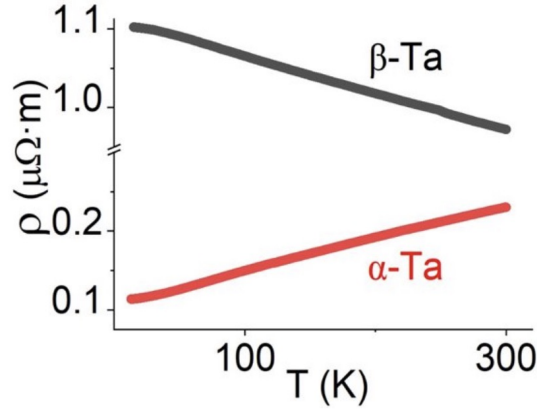
Figure 1.1: Resistivity vs. temperature plot for a β-Ta and a α-Ta: a negative Temperature Coefficient of Resistivity (TCR) is shown for the black data points (beta-phased Tantalum thin film)

1.2.2 Johnson-Nyquist Noise

Thermal noise, also known as Johnson-Nyquist noise, arises from the thermal agitation of charge carriers in a conductor. Unlike shot noise (SN), which depends on the discrete nature of electron and an applied current, thermal noise is present even in the absence of bias current.

In the measurement setup, the total noise is a superposition of SN and thermal noise, and its voltage noise spectral density S_V can be expressed as:

$$S_V = 2FeR(V \coth \frac{V}{V_{th}} - V_{th}) + 4k_B TR \tag{1.1}$$

Here, F is the Fano factor, e is the elementary charge, and V_{th} is the thermal broadening voltage bias, determining the crossover region between thermal noise and SN [1]. At low bias, $V_B << V_{th}$, the second term in equation (1.1) dominates, so the system is governed by thermal noise, $S_{V,th} = 4k_B TR$. At higher bias, $V_B >> V_{th}$, SN becomes dominant and exhibits a linear dependence, as shown by the red line on the left side of Figure 1.2.

By focusing on thermal noise, this study uses the differential noise measurement approach to derive a formula for the thermal conductivity through the leads connecting the β-Ta strip. The differential noise measurement takes the derivative of total noise with respect to current bias. Figure 1.2 shows the total noise and its derivative noise diagram for 500nm β-Ta strip at cryogenic temperature 4.3K. As will be discussed in Chapter 2 (Methods), LabVIEW does not directly output noise power but rather a voltage value. For details on how this voltage output was converted into voltage noise power, see Appendix A.2.
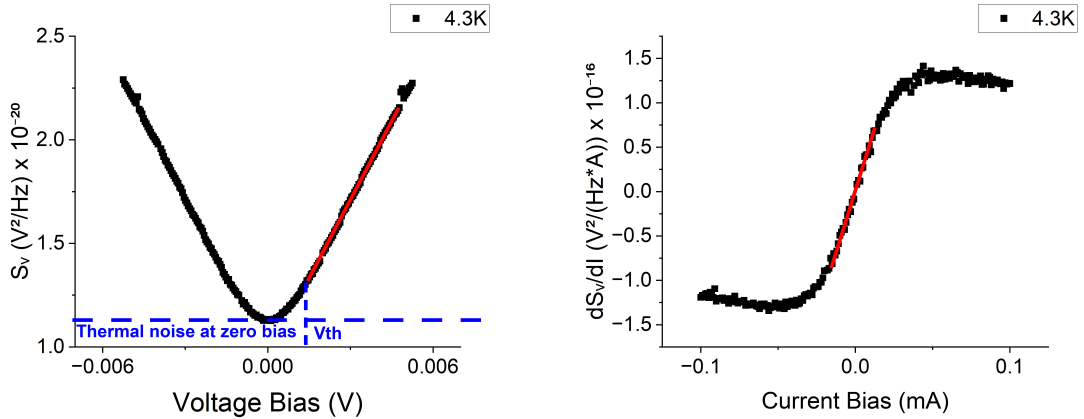
Figure 1.2: **Left**: converted total noise power (S_V) vs. voltage bias for a 500 nm β-Ta strip. The horizontal blue dotted line shows the thermal noise when the voltage bias is zero while the vertical blue dotted line refers to the crossover voltage bias V_{th}; **Right**: converted differential total noise power ($\frac{dS_V}{dI}$) vs. current bias for a 500 nm β-Ta strip(at cryogenic temperature). The y-axis is the derivative of noise power with respect to current bias in unit $\left[\frac{V^2}{Hz \cdot A}\right]$.

1.2.3 Heat Conduction

Heat conduction refers to the transfer of thermal energy between regions of matter driven by a temperature gradient. In our system, the temperature gradient arises due to the applied current, and heat is conducted through both the β-Ta strip and the copper leads. Using the differential noise measurement described above, we can derive the thermal conductivity. Following a closely related result derived in Section 5.2 of Dames (2013) [4], the steady-state temperature rise due to Joule heating in a suspended thin film can be estimated using a parabolic temperature profile, yielding the relation:

$$T = T_0 + \frac{QL}{3\kappa A} \tag{1.2}$$

where T is the average temperature, T_0 is the ambient (bath) temperature, Q is the power dissipated, L is the conductor length, κ is the thermal conductivity, and A is the cross-sectional area. This expression assumes uniform volumetric heating, steady-state one-dimensional conduction, constant thermal conductivity, and symmetric thermal boundary conditions.

Furthermore, in Figure 1.2, the linear region of differential noise measurements occurs within the thermal broadening region, where $V_B < |V_{th}|$. Based on this, we made a critical assumption that the measured noise is entirely thermal in origin. Using the slope of the converted differential noise data, as described in Appendix A.2, $\frac{dS_V}{dI}/I$, the thermal conductivity κ can be expressed as shown in Equation (1.3).

$$\kappa = \frac{8R^2 L k_B}{3A(\frac{dS_V}{dI}/I)} \tag{1.3}$$

A thorough derivation of equation is shown in Appendix A.1. Overall, by analyzing the slope of the differential thermal noise with respect to current, one can derive an expression for κ that reflects the electronic heat transport through the leads.

1.2.4 Heat Dissipation

While heat conduction introduces how thermal energy transports through a material, heat dissipation tells us how energy is removed from a system, typically through a combination of conduction, layer interface transfer, or radioactive and convective losses. In a nanoscale system that is kept under cryogenic temperature 4.3K, low temperature models have to be considered for electrons and phonons contribution in thermal dissipation. Along with the models, we decided to use thermal conductivity κ as the parameter to explore heat dissipation in β-Ta.

Wiedemann-Franz Law and Debye's Model

For the electronic contribution, the Wiedemann–Franz law relates the electrical conductivity σ and thermal conductivity κ via the Lorentz number L, as expressed in Equation (1.4). Although originally inspired by the classical Drude model—which treats conduction electrons as a gas of free particles scattering off relatively immobile ions—the Wiedemann–Franz law is more rigorously justified through quantum models such as the Sommerfeld theory of electrons. These models consider the Fermi-Dirac distribution of electrons and show that, at low temperatures, κ exhibits a linear dependence on temperature, consistent with the behavior predicted by the Wiedemann–Franz law.

$$\frac{\kappa}{\sigma} = LT \tag{1.4}$$

Another pathway for heat dissipation through the β-Ta strip is via phonons. In estimating the phonon contribution to the specific heat of a solid, the Debye model correctly captures the experimentally observed T^3 temperature dependence at low temperatures [7].

Fitting Equation

Thus, for local thermal equilibrium, a simple fitting function of the thermal conductivity is given by the sum of contributions from electrons and lattice vibrations, as shown in Equation (1.5).

$$\kappa = aT + bT^3 \tag{1.5}$$

However, heat dissipation through phonons escaping from the metal into the substrate made of sapphire is a different story. As an insulating material, sapphire (Al_2O_3) introduces thermal non-equilibrium at the interface. As a result, the simple additive model of thermal conductivity, $\kappa = aT + bT^3$, which assumes local thermal equilibrium through the metal, cannot be used to accurately describe heat dissipation into the substrate.

Chapter 2

Experimental Work

2.1 Methods

To investigate the thermal transport behavior of β-Ta, the author conducted a differential noise measurement on nanoscale β-Ta strips deposited on sapphire substrates. The nanowires were fabricated using multi-step electron beam lithography (EBL) and UHV sputtering techniques to define precise geometries and interfaces.

Initially, resist layers of MMA EL6 and PMMA 495 were spin-coated at 7000 rpm onto the sapphire chip, and patterns were written using EBL based on the design files from DesignCAD. The exposed region then underwent chemical development to reveal the intended structure. Then, metal depositions were performed after each EBL step. Precise control over the fabrication parameters ensured accurate pattern transfer onto the sapphire chip. In Figure 2.1, a schematic cross-section of the β-Ta nanowire is shown. Each strip consisted of a 10 nm β-Ta layer connected by titanium/copper leads, with a thin 2 nm Ti(2) layer as the metal adhesion promoter and a 2 nm aluminum oxide $AlO_x(2)$ cap to prevent oxidation of the metal strip.

Figure 2.2 presents the scanning electron microscopy (SEM) images of the fabricated β-Ta nanowire that has 500nm in length, 1500nm in width, and 10nm in thickness.
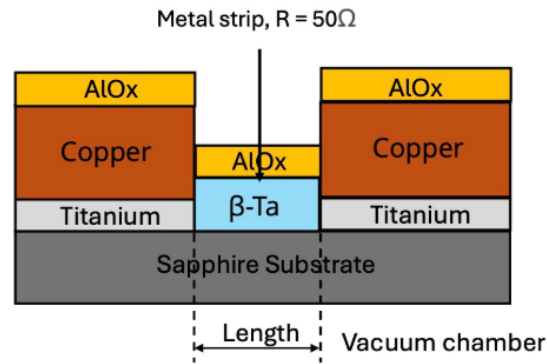
Figure 2.1: Schematic cross section of the β-Ta chip. Leads are sputtered in the following order: Ti(1)/Cu(60).
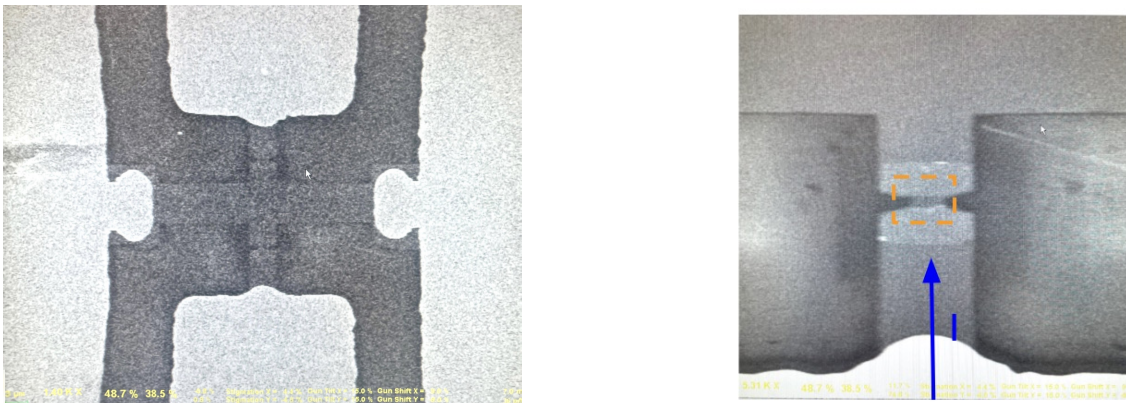
Figure 2.2: **Left**: SEM image of the leads and the β-Ta strip; **Right**: magnified SEM image of the flare-out design for precise β-Ta strip geometry. The length of the β-Ta strip is 500 nm, width is 1500 nm, and thickness is 10 nm. (Orange rectangle: circles out β-Ta strip; blue line: the direction that current flows)

After finalizing the fabrication of β-Ta nanowires, noise measurements were performed under a cryogenic temperature starting at 4.3 K in a microwave cryostat. To avoid impedance mismatch, the sample resistance is controlled between $45 - 55\Omega$ by keeping the width-length ratio constant. To start with, a DC bias was applied to the sample, and the corresponding noise was extracted using a bias tee. The separated noise then underwent three ultra-low noise amplifiers to amplify the noise. The amplifiers acted as band passes for microwave frequency range noise, and we could observe the frequency peak at 350 MHz after passing through an amplifier.

For differential noise measurements, the lock-in amplifier was used to measure the derivative of noise with respect to the current bias. Overall, we could extract our data from LabVIEW and convert them to noise power following Appendix A.2. A specific setup image can be found in Figure 2.3.
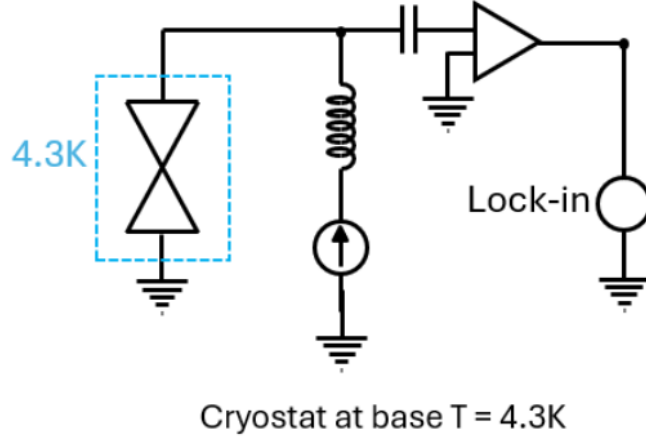
Figure 2.3: Schematics of the differential noise measurement setup: cryogenic temperature is set at 4.3 K as the base temperature. (The blue dashed line shows the cryostat is kept under base temperature)

2.2   Results and Discussion

Strips with lengths ranging from 100 nm to 2 μm were thoroughly measured, providing a sufficient range to observe variations in electronic and phononic contributions. By combining Equation (1.3) with fitting Equation (1.5), we extracted the electron and phonon contribution coefficients, a and b, through nonlinear curve fitting in Origin7. Notably, the analysis used the inverse form of the fitting equation shown in Figure 2.4. This approach was chosen because the uncertainty in the differential noise appears in the denominator of Equation (1.3); inverting then helps mitigate error propagation. Additional fitting results for various lengths are presented in Appendix A.3.

Table 2.1 summarizes the fitted parameters a and b, representing the respective
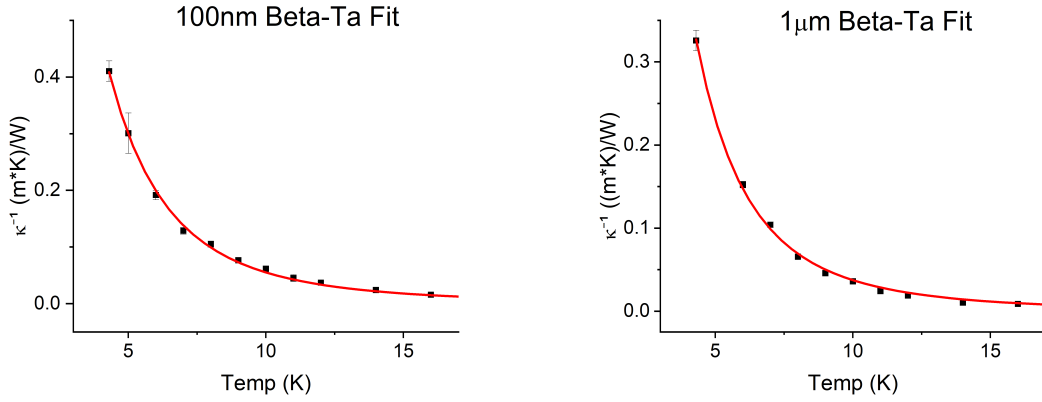
Figure 2.4: **Left**: an inverse of thermal conductivity κ^{-1} vs. temperature, ranging from 4.3 K to 16 K, for a 100 nm β-Ta (10); **Right**: an inverse of thermal conductivity κ^{-1} vs. temperature, ranging from 4.3 K to 16 K, for a 1 μm β-Ta (10).

Length (nm)	a (W/(m·K^2))	b (W/(m·K^4))
100	0.287 ± 0.017	0.0153 ± 0.0007
500	0.213 ± 0.010	0.0066 ± 0.0004
1000	0.270 ± 0.074	0.0219 ± 0.0032
2000	-0.161 ± 0.073	0.0801 ± 0.0035

Table 2.1: Fitted thermal conductivity parameters for β-Ta strips of different lengths.

contributions from electrons and phonons in heat transport through the metallic leads. For 100 nm, 500 nm, and 1 μm lengths, the electron contribution remains relatively steady, with a slight dip observed in the 500 nm sample. However, as shown in Figure 2.5, the 2 μm sample displayed an anomalous negative electron contribution, suggesting potential limitations of the current model.

One plausible explanation is that the phonon contribution was underestimated by assuming a T^3 at low temperatures. In reality, boundary scattering may cause deviations from this cubic trend. If the actual phonon contribution follows a higher-order dependence T^n, where $n > 3$, forcing a T^3 fit may artificially inflate the phonon term and result in a spurious negative electron term.

The anomalous behavior of the electron contribution in the 2 μm sample, particularly the negative value presented, suggests that our general model can not fully capture
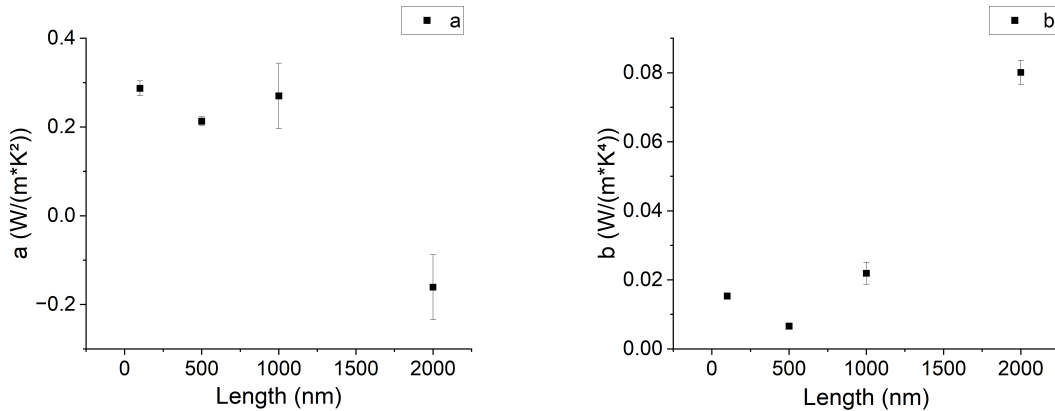
Figure 2.5: **Left**: electron contribution coefficient (a) vs. length at cryogenic temperature 4.3 K. ; **Right**: phonon contribution coefficient (b) vs. length at cryogenic temperature 4.3 K. The contribution coefficients at 2 μm draws our attention as its electron contribution is negative, suggesting a possible breakdown of the thermal conductivity model in Equation (1.5).

the thermal dissipation mechanisms at longer scales. In particular, $\kappa = aT + bT^3$ only describes the heat conduction through metallic leads at a local thermal equilibrium, where both electron and phonon contributions are described by a single temperature field. However, this model does not account for heat dissipation into the insulating sapphire substrate, which becomes increasingly relevant at longer strip lengths. To explore these additional dissipation pathways and visualize the spatial temperature distribution in the system, we turned to numerical simulations using COMSOL Multiphysics.

Chapter 3

COMSOL Simulation

3.1 Motivation

While experimental measurements revealed key properties of thermal transport through the metallic leads of β-Ta nanostructures, they do not directly capture the heat flow into the sapphire substrate. This is particularly important, as electrons dominate heat conduction at cryogenic temperatures over short length scales, but phonon escape through the substrate becomes more significant as the strip length increases. Unfortunately, the thermal conductivity estimation model $\kappa = aT + bT^3$ primarily accounts for heat dissipation through the copper leads under local thermal equilibrium.

Therefore, to address this limitation and complement the experimental measurements, we designed a three-dimensional Joule heating simulation model, using COMSOL Multiphysics, for qualitative and visual analysis. The model provides insights into the spatial distribution of temperature and how the temperature of the β-Ta metal strip varies with current bias.

3.2   Methods

The COMSOL model used in this work draws inspiration from a simulation framework previously developed by a former PhD student in our group [2]. Building on that foundation, I adapted the model to match the geometry, materials, and boundary conditions relevant to the β-Ta nanostrip system studied here.

   The COMSOL model consists of a β-Ta strip (1 μm and 100 nm) connected by two copper leads and mounted on a sapphire substrate, as shown in 3.1. Electrical and thermal parameter values for Cu and Al_2O_3 follow the literature value [5]. For β-Ta, the thermal conductivity is set to follow the experimentally derived form $\kappa = aT + bT^3$. Joule heating from a DC bias serves as the heat source in the model, and the cryostat is treated as a thermal reservoir held at 4.3 K.

   Next, thermal and electrical boundary conditions were applied to define the current source and initial temperature of the system. Fine meshing was implemented to divide the 3D model into smaller, discrete elements, improving the accuracy of simulation results. Further details of setting up a COMSOL simulation are shown in Appendix A.4.
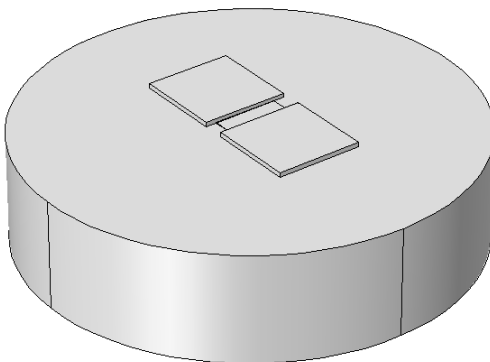
Figure 3.1: COMSOL 3D Joule heating model: one sapphire substrate, two copper leads, and one β-Ta strip of length 1 μm. Parameters such as thermal conductivity κ, and electrical conductivity σ strictly follow the experimental values.

3.3 Result and Discussion

Implementing a stationary Joule heating simulation allows us to extract useful results, including qualitative temperature distribution plots (cross-sections) and integrated temperature profiles under various current biases.

3.3.1 Thermal Boundary Resistance

By isolating the leads and substrate contribution in COMSOL, the simulation result confirmed that heat generated in the β-Ta strip was not confined to metallic leads dissipation - this is evident from a higher average temperature shown on the β-Ta strip when only lead dissipation is considered. When substrate became involved in the system, a key parameter – thermal contact resistance – influenced the thermal transfer between the metal strip and the sapphire substrate. Thermal boundary resistance at the interfaces between two solids, metal and dielectric, can be understood through two limiting models: the acoustic mismatch model and the diffuse mismatch model. Thermal boundary resistance is crucial because phonons are sensitive to surface defects, which significantly affect interfacial conductance, particularly for longer samples where phonon transport dominates [9].

3.3.2 COMSOL Simulation

Although temperature distribution alone does not directly quantify electron and phonon contributions to heat dissipation, Figure 3.2 provides a qualitative visualization: phonons tend to escape through the substrate in longer β-Ta strips.

To further evaluate this dissipation pathway, we plotted temperature versus current bias using COMSOL data, as shown in Figure 3.3. By recording the average temperature of the β-Ta strip across current bias increments from $-0.5\,\mathrm{mA}$ to $0.5\,\mathrm{mA}$,
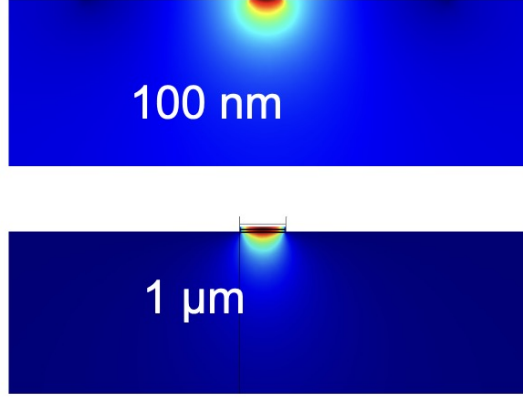
Figure 3.2: Cross-sectional temperature distribution plot for 100 nm and 1 μm β-Ta strip when a current bias of 0.5 mA is applied.

we computed a COMSOL simulated thermal noise spectral density using:

$$S_{V,th} = 4k_B TR$$

Since we assumed that thermal noise dominates throughout noise measurement, comparing COMSOL-simulated noise and experimental noise value is justified. Figure 3.3 shows the simulated thermal noise (temperature-dependent noise power) for the 100 nm and 1 μm samples. A difference of approximately 33.3% is observed between the two, with the shorter sample exhibiting a value of around 4×10^{-20} V^2/Hz, compared to approximately 3×10^{-20} V^2/Hz for the longer sample at a current bias of 1 mA. This reduction in thermal noise for the longer sample reflects enhanced phonon escape into the substrate, which becomes a more dominant dissipation pathway as the device length increases.

Theoretically, the expected thermal noise generated from the COMSOL simulation should align with our experimental values, at least the thermal broadening region, as the parameters input strictly adhere to the experimental outputs. However, a consistently lower noise power is observed across all ranges of applied current bias.
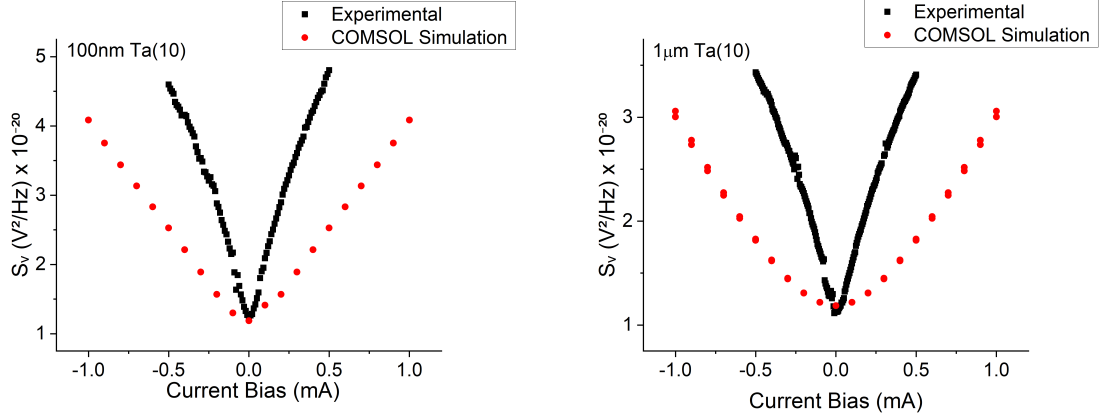
Figure 3.3: **Left**: COMSOL simulated noise power vs. experimental noise power on a 100nm β-Ta strip; **Right**: COMSOL simulated noise power vs. experimental noise power on a 1μm β-Ta strip. Both plots highlight a systematic underestimation of simulated noise.

3.3.3 Limitations and Future Work

One limitation of the COMSOL simulation is that it does not account for the temperature difference between electrons and phonons, which can arise due to hot-electron effects during Joule heating [8]. In reality, electron-phonon relaxation can introduce nonequilibrium behavior, especially in nanoscale systems. However, in our model, the thermal conductivity $\kappa = aT + bT^3$ was directly derived from experimental measurements and used as input, meaning the simulated average temperature—and thus the thermal noise—should still match experimental results under steady-state conditions. Therefore, while the lack of a two-temperature model in COMSOL is a general limitation, it does not explain the systematic underestimation of thermal noise observed in our results. This discrepancy may instead stem from other modeling simplifications, such as the assumed boundary conditions or mesh resolution.

For future work, a two-temperature model is necessary for quantifying the potential effects of electron-phonon relaxation in systems where hot-electron phenomena are expected to play a significant role. This could be achieved by Python or MATLAB, allowing separate calculations on electron and phonon temperature dynamics through coupled differential equations. Additionally, investigating longer samples exceeding

$2\,\mu m$ should be evaluated to determine whether the observed outlier behavior is systematic or simply a consequence of poor sample data quality. Finally, examining shorter samples such as the nanopillars with lengths of $4\,nm$, $8\,nm$, and $20\,nm$, as studied by our group, may reveal whether dimensional confinements change the balance between phonon and electron contributions in heat dissipation.

Chapter 4

Conclusion

To summarize my honor thesis research, ultrathin films of β-Ta with lengths ranging from $100\,\text{nm}$ to $2\,\mu\text{m}$ were produced, and the experimental setup and analysis for differential noise measurements were presented. We explored thermal dissipation in β-Ta nanostructures at cryogenic temperature 4.3 K through experiment measurements and COMSOL simulation. By restricting our analysis to the thermal broadening region, we adopted the simplifying assumption that all measured noise is thermal.

From the differential noise measurements, a simple equation $\kappa = aT + bT^3$, separating the electron and phonon contribution, was built from Wiedemann-Franz Law and Debye's model for the thermal conductivity through metallic leads. This led to the extraction of the electron and phonon contribution coefficients. We see a relative constant contribution from electrons and phonons through the metallic leads, although an unexplainable outlier was observed in the $2\,\mu\text{m}$ sample under the low-temperature model. Acknowledging the limitation of this model in analyzing heat dissipation through the insulating substrate, we employed a COMSOL Multiphysics modeling software and utilized the Joule heating model. Our theoretical work illustrates the temperature distribution under specific boundary conditions should yield simulated thermal noise values that are comparable to the experimental results. However, the

simulated result underestimated the thermal noise across all biases which we could not explain.

In conclusion, this study enhances our understanding of heat dissipation in a bad metal β-Ta, an anomalous material that exhibits increasing relevance to spintronics and nanoelectronics. The method and the insights presented could serve as a foundation for further investigations into thermal transport in a bad metal.

Appendix A

Appendix

A.1 Full Derivation of Thermal Conductivity

Here is the full derivation of how thermal conductivity is calculated through shot noise. It all starts from the heat conduction equation:

$$T = T_0 + \frac{QL}{3\kappa A}$$

T represents the temperature, Q is the thermal power, and we can substitute with $I^2 R$ For our measurement setup, we need to take account of the lock-in amplifier. To convert the voltage output into the noise power, we could write the following equation.

$$\frac{dS_V}{dI} = C \cdot \frac{dV}{dI} \tag{A.1}$$

C is the conversion factor to convert voltage output into noise voltage power shown in Appendix A.2 Equation (A.3). By taking the derivative of noise voltage power with respect to the current in equation (1.1),

$$S_V = 2FeR(V \coth \frac{V}{V_{th}} - V_{th}) + 4k_B T R$$

$$\frac{dS_V}{dI} = 4k_B R_s \frac{d}{dI}\left(\frac{I^2 R_s L}{3\kappa A}\right)$$

$$\frac{dS_V}{dI} = \frac{8I R_s^2 L k_B}{3\kappa A}$$

Utilizing equation (A.1),

$$\frac{dV}{dI} = \frac{8I R_s^2 L k_B}{3\kappa A C}$$

Rearranging the equation and applying the conversion factor C gives us thermal conductivity in terms of the differential noise $\frac{dS_V}{dI}$, so we achieved our final equation (1.3).

$$\kappa = \frac{8R^2 L k_B}{3A\left(\frac{dS_V}{dI}/I\right)}$$

R_s is the sample resistance. Within our experiment, there is also the lead resistance on the chip R_l, and the line resistance R_L that is constant at 50Ω. From the differential dataset from LabVIEW, I took the slope of the thermal broadening region $\frac{dS_V}{dI}/I$ and calculated the conversion factor.

A.2 Processing LabVIEW Output for Noise Analysis

In this section, we detail the procedure for converting the voltage output recorded in LabVIEW into actual thermal noise power, which was necessary for calculating thermal conductivity based on the differential noise slope. We will be using the resistance values for our 500 nm β-Ta sample.

Constants and Resistances

$$R_s = \text{Sample resistance} = 52.5 \ \Omega$$

$$R_l = \text{Lead resistance on the chip} = 2.5 \ \Omega$$

$$R_L = \text{Line resistance (load)} = 50 \ \Omega$$

Johnson Current Noise Power into a Short

The Johnson current noise power produced by the sample and leads into a short is:

$$S_{sl} = \frac{4k_B T}{R_s + R_l}$$

Johnson Current Noise Power into the Load

$$S_{II,\text{meas}} = \frac{S_{sl}}{\left(1 + \frac{R_L}{R_s + R_l}\right)^2} = \frac{4k_B T(R_s + R_l)}{(R_s + R_l + R_L)^2}$$

Johnson Voltage Noise Power into the Load

$$S_{VV,\text{meas}} = S_{sl} \left(\frac{R_L}{R_s + R_l + R_L}\right)^2 = 4k_B T(R_s + R_l) \left(\frac{R_L}{R_s + R_l + R_L}\right)^2$$

With numeric values:

$$S_{VV,\text{meas}} = 0.03175\,[\text{V/K}] \cdot T(K) \cdot (\text{meas.uni}) = 4 \cdot 1.38 \times 10^{-23} \cdot T(K) \cdot 55 \cdot \left(\frac{50}{50 + 52.5 + 2.5}\right)^2$$

$$0.03175\,[V] \cdot (\text{meas.uni}) = 6.884 \times 10^{-22}\,[V^2/Hz]$$

Thus, we can calculate the exact value for 1 measurement unit in units of $\left[\frac{V}{Hz}\right]$, and we eventually know that 1 measurement unit is equivalent to 2.168×10^{-20} $V^2/$Hz at the amplifier.

$$1 \text{ measurement unit} = 2.168 \times 10^{-20} \text{ V/Hz}$$

$$\text{Amplifier noise offset} = 1.687 \text{ V}$$

The coefficient 0.03175 [V/K] was extracted as the slope of the thermal noise versus temperature plot, while the amplifier noise offset was obtained from the y-intercept of the same linear fit.

Finite Bias: Johnson + Shot + Amplifier Noise

Voltage noise from the sample and leads into an open circuit:

$$S_{V,s} = \text{Voltage noise from sample (open circuit)}$$

$$S_{V,l} = 4k_B T R_l \quad \text{(from leads)}$$

Leads contribute noise to the amplifier:

$$S_{V,\text{leads,amp}} = 0.03175 \cdot \frac{R_l}{R_s + R_l} \cdot T(K) = 1.443 \times 10^{-3} \cdot T(K)$$

Now we could remove the leads contribution and amplifier offset from our measured

noise S_{meas} and utilized the conversion factor calculated from above. The factor $\left(\frac{R_s+R_l+R_L}{R_L}\right)^2$ is used to recover the open-circuit voltage noise produced by the sample from the measured noise at the amplifier input, by compensating for the voltage division caused by the total resistance in the circuit.

$$S_V = [S_{\text{meas}} - 1.687 - 1.443 \times 10^{-3} \cdot T] \cdot 2.168 \times 10^{-20} \cdot \left(\frac{R_s + R_L + R_l}{R_L}\right)^2 \quad \text{(A.2)}$$

Equation (A.2) is the final equation for converting a LabVIEW voltage output into a voltage noise power in unit V^2/Hz. For differential noise power conversion, we take the derivative with respect to current bias to Equation (A.2); therefore, we could easily derive Equation (A.3), which is the conversion equation for differential voltage noise power shown in Figure 1.2. Moreover, we can generalize the total conversion factor into a variable called C, and it can expressed as:

$$C = \text{meas.uni} \cdot \left(\frac{R_s + R_L + R_l}{R_L}\right)^2$$

$$\frac{dS_V}{dI} = \left(\frac{dS_{\text{meas}}}{dI}\right) \cdot 2.168 \times 10^{-20} \cdot \left(\frac{R_s + R_L + R_l}{R_L}\right)^2 \quad \text{(A.3)}$$

A.3 Thermal Conductivity Fitting Results for all Lengths
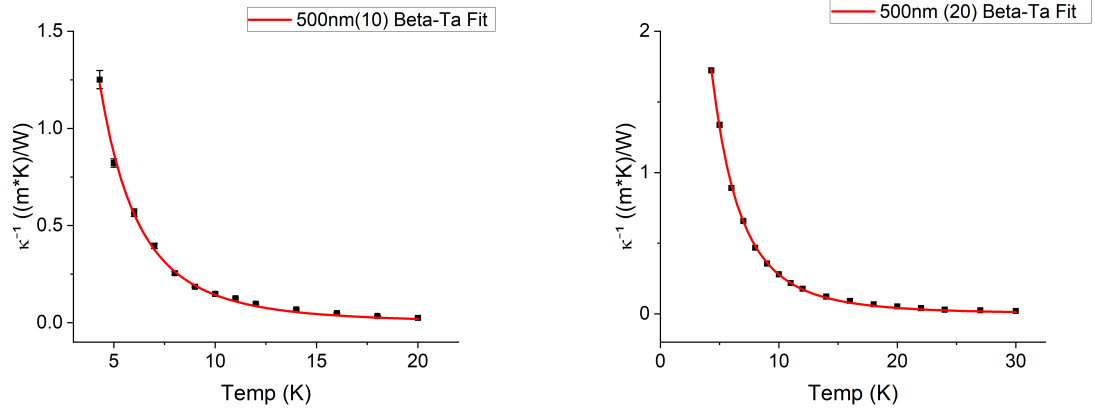

Figure A.1: Left: thermal conductivity fit for 500nm β-Ta (10); Right: thermal conductivity fit for 500nm β-Ta (20).
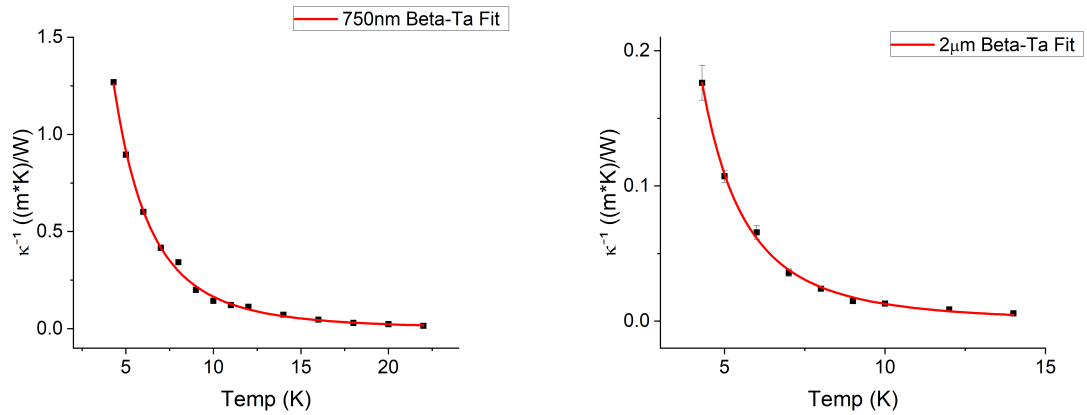

Figure A.2: Left: thermal conductivity fit for 750nm β-Ta(10); Right: thermal conductivity fit for 2 μm β-Ta(20).

A.4   COMSOL Simulation
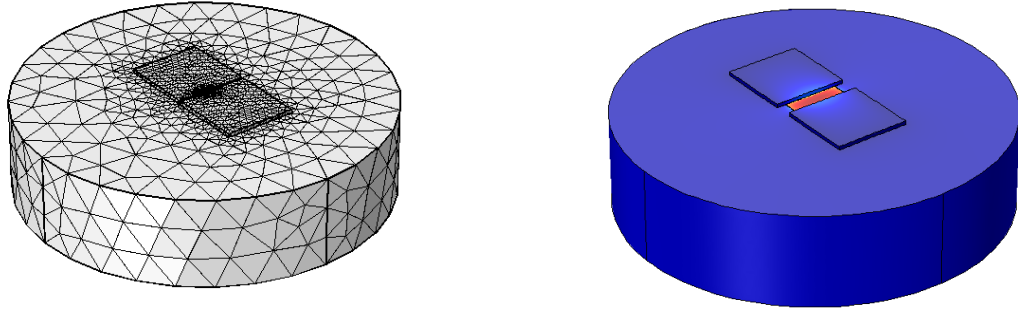
Figure A.3: Left: meshing of COMSOL Simulation model. Fine meshing was implemented to ensure the average temperature and temperature profile of the model are precise; Right: a COMSOL simulation image showing the temperature distribution for the model after heating up by current bias applied.
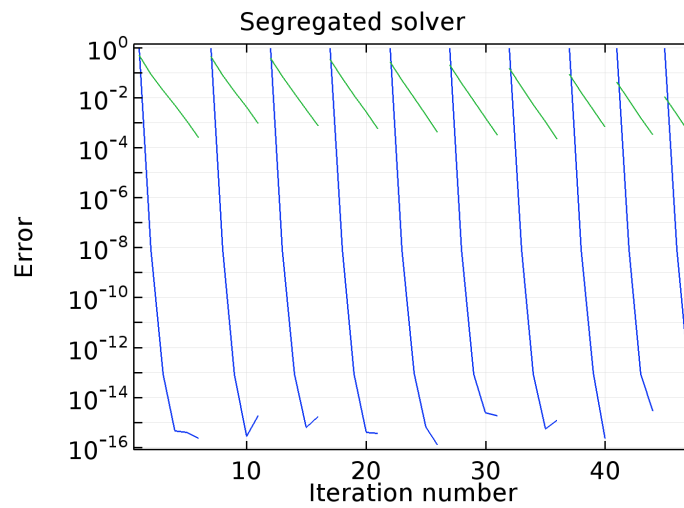

Figure A.4: Error of the Joule heating model converges at 10^{-15}. The COMSOL simulation studies the model at this level of error, enhancing preciseness of the analysis result.

Bibliography

[1] Ya.M. Blanter and M. Büttiker. Shot noise in mesoscopic conductors. *Physics Reports*, 336(1–2):1–166, Sep 2000. doi: 10.1016/s0370-1573(99)00123-4.

[2] Guanxiong Chen and Sergei Urazhdin. Transport and relaxation of current-generated nonequilibrium phonons from nonlocal electronic measurements. *Physical Review B*, 105(10), Mar 2022. doi: 10.1103/physrevb.105.l100302.

[3] Debanjan Chowdhury, Antoine Georges, Olivier Parcollet, and Subir Sachdev. Sachdev-ye-kitaev models and beyond: Window into non-fermi liquids. *Reviews of Modern Physics*, 94(3), Sep 2022. doi: 10.1103/revmodphys.94.035004.

[4] Chris Dames. Measuring the thermal conductivity of thin films: 3 omega and related electrothermal methods. *Annual Review of Heat Transfer*, 16, 2013.

[5] Elena R. Dobrovinskaya, Leonid A. Lytvynov, and Valerian Pishchik. Properties of sapphire. *Sapphire*, page 55–176, 2009. doi: 10.1007/978-0-387-85695-7_2.

[6] N. N. Kovaleva, D. Chvostova, A. V. Bagdinov, M. G. Petrova, E. I. Demikhov, F. A. Pudonin, and A. Dejneka. Interplay of electron correlations and localization in disordered beta-tantalum films: Evidence from dc transport and spectroscopic ellipsometry study. *Applied Physics Letters*, 106(5), Feb 2015. doi: 10.1063/1.4907862.

[7] Steven H. Simon. *The Oxford Solid State Basics*. Oxford University Press, 2019.

[8] Andrew H. Steinbach, John M. Martinis, and Michel H. Devoret. Observation of hot-electron shot noise in a metallic resistor. *Physical Review Letters*, 76(20): 3806–3809, May 1996. doi: 10.1103/physrevlett.76.3806.

[9] E. T. Swartz and R. O. Pohl. Thermal boundary resistance. *Reviews of Modern Physics*, 61(3):605–668, Jul 1989. doi: 10.1103/revmodphys.61.605.

[10] M. Szurek, H. Cheng, Z. Pang, Y. Zhang, J. Bacsa, and S. Urazhdin. Anomalous shot noise in a bad metal beta-tantalum, 2024. URL `https://arxiv.org/abs/2410.18349`.